



**PLAXIS**

**The SHANSEP MC model**

**2016**

*Edited by:*

S. Panagoulas  
*PLAXIS bv, The Netherlands*

F. Palmieri  
*PLAXIS bv, The Netherlands*

R.B.J. Brinkgreve  
*Delft University of Technology & PLAXIS bv, The Netherlands*

**TABLE OF CONTENTS**

|          |  |           |
|----------|--|-----------|
| <b>1</b> | <b>Introduction</b>  | <b>5</b>  |
| 1.1      | Normalized behaviour and the SHANSEP concept                       | 5         |
| <b>2</b> | <b>The SHANSEP MC constitutive model</b>                           | <b>7</b>  |
| 2.1      | Model Parameters   | 7         |
| 2.2      | On the use of the SHANSEP MC model                                 | 11        |
| 2.3      | Modelling the undrained behaviour                                  | 12        |
| 2.4      | The SHANSEP MC model in combination with other constitutive models | 14        |
| <b>3</b> | <b>Verification - triaxial compression tests</b>                   | <b>17</b> |
| <b>4</b> | <b>Practical Applications</b>                                      | <b>21</b> |
| 4.1      | Fluctuation of the phreatic level                                  | 21        |
| 4.2      | Embankment construction on soft clay                               | 25        |
| 4.3      | The SHANSEP MC and the Soft Soil Creep model                       | 29        |
| <b>5</b> | <b>Conclusions</b>   | <b>31</b> |
| <b>6</b> | <b>References</b>  | <b>33</b> |



## 1 INTRODUCTION

The SHANSEP MC model (Stress History and Normalized Soil Engineering Properties) constitutes a soil model implemented in PLAXIS, intended for undrained soil loading conditions. It is based on the linear elastic perfectly-plastic Mohr-Coulomb model, but modified such that it is able to simulate potential changes of the undrained shear strength  $S_u$  based on the effective stress state of the soil. It takes into account the effects of stress history and stress path in characterizing soil strength and in predicting field behaviour.

### 1.1 NORMALIZED BEHAVIOUR AND THE SHANSEP CONCEPT

Laboratory tests conducted at the Imperial College using remolded clays (Henkel (1960) and Parry (1960)) and at the Massachusetts Institute of Technology on a wide range of clays, give evidence that clay samples with the same over-consolidation ratio (*OCR*), but different consolidation stress  $\sigma'_c$  and therefore different pre-consolidation stress  $\sigma'_{pc}$ , exhibit very similar strength and stress-strain characteristics when the results are normalized over the consolidation stress  $\sigma'_c$ .

Figure 1.1 illustrates idealized stress-strain curves for isotropically consolidated undrained triaxial compression test on a normally-consolidated clay, with consolidation stresses  $\sigma'_c$  of 200 kPa and 400 kPa. As depicted in Figure 1.2, the stress-strain curves are plot on top of each other when they are normalized over the consolidation stresses.

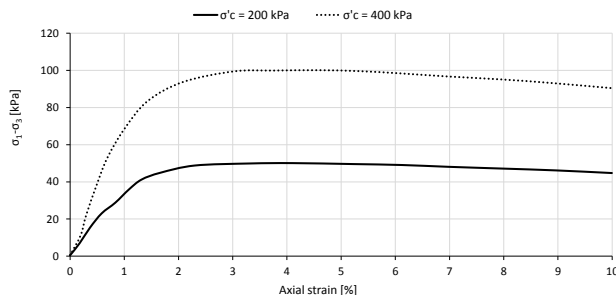


Figure 1.1 Triaxial compression test data of homogeneous clay (Ladd & Foott, 1974)

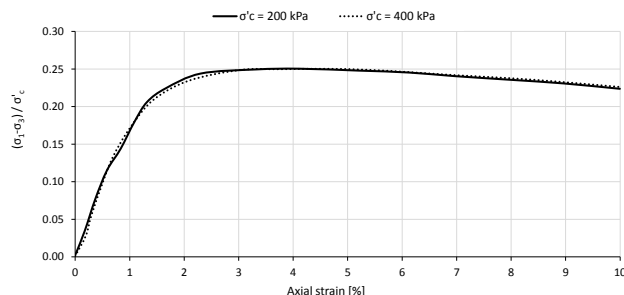


Figure 1.2 Normalized triaxial compression test data of homogeneous clay (Ladd & Foott, 1974)

In practice, normalized behavior is not as perfect as shown in Figure 1.2. Usually, there is

discrepancy in the normalized plots caused by different consolidation stresses, soil deposit heterogeneity or even the fact that the conditions from one soil test to another are not identical. However, this discrepancy is reported to be quite small (Ladd & Foott, 1974) and as a result the observed normalized soil behaviour is adopted in engineering practice. It is worth mentioning that tests on quick clays and naturally cemented soils, which have a high degree of structure, will not exhibit normalised behaviour because the structure is significantly altered during the deformation process (Ladd & Foott, 1974).

The observations of normalised soil behaviour lead to the Normalised Soil Parameter (NSP) concept. According to NSP, Figure 1.3 illustrates data from Ladd & Foott (1974) which show the variation of the undrained shear strength  $S_u$  normalised over the current vertical effective stress  $\sigma'_{v0}$  against the over-consolidation ratio  $OCR$ , for five cohesive soils, in correspondence with their index properties. The data show a similar trend of increasing  $S_u/\sigma'_{v0}$  with  $OCR$ .

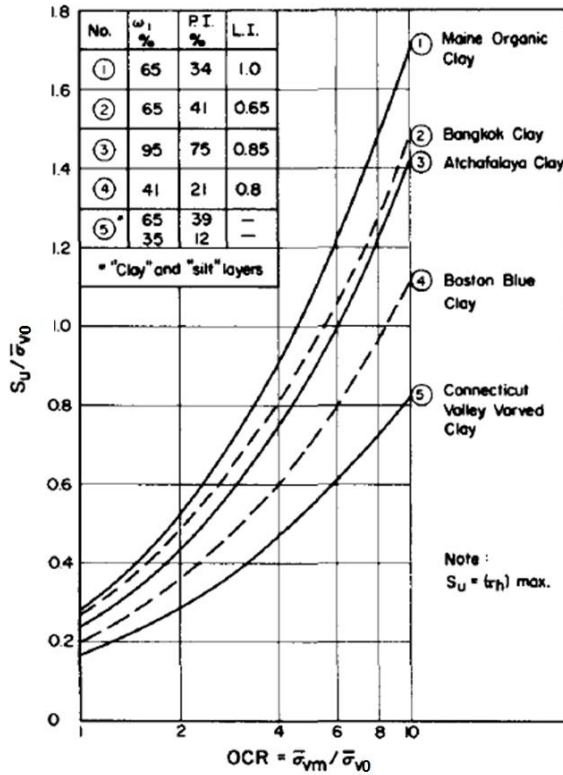


Figure 1.3 Variation of  $S_u/\sigma'_{v0}$  with  $OCR$  for five different clays (Ladd & Foott, 1974)

## 2 THE SHANSEP MC CONSTITUTIVE MODEL

Stress History and Normalised Soil Engineering Properties (SHANSEP) is the basis of the constitutive model hereby presented. The stress history of the soil deposit can be evaluated by assessing the *OCR* variation via the current and the pre-consolidation stress profiles. Based on the NSP concept, the undrained shear strength  $S_u$  is estimated as:

$$S_u = \alpha \sigma'_{v0} \left( \frac{\sigma'_{1,max}}{\sigma'_{1}} \right)^m = \alpha \sigma'_{v0} (OCR)^m \quad (2.1)$$

in which  $\alpha$  and  $m$  are normalised soil parameters.

The model is implemented in PLAXIS such that the effective major principal stress  $\sigma'_1$  is considered to compute the *OCR*. This is thought to be a more objective parameter in comparison with the vertical effective stress  $\sigma'_v$ , as it is the most compressive value, independent of the Cartesian system of axes. Assuming horizontal soil layering, both parameters would result in the same value of *OCR*. However, if the vertical effective stress  $\sigma'_v$  was considered in case of soil slopes, the rotation of principal axes for soil elements adjacent to the slope would result in slightly lower values of *OCR*.

### 2.1 MODEL PARAMETERS

The SHANSEP MC model is formulated such that it initially behaves as the Mohr-Coulomb model until it is switched to the SHANSEP concept by the user (see Section 2.2). It should be preferably used in combination with undrained behaviour. For user-defined soil models, undrained behaviour is available as the Undrained (A) drainage type. However, this drainage type can be ignored before switching to the SHANSEP concept by using the calculations option *Ignore undrained behaviour* in the *Phases* window. After switching to the SHANSEP concept, the model behaves according to the Undrained (B) drainage type.

Since the SHANSEP MC model is an extension of the linear-elastic perfectly-plastic Mohr-Coulomb model, the model parameters can be classified in two groups, i.e. the Mohr-Coulomb model parameters and the SHANSEP parameters. For the 'pre-switching' behaviour only the Mohr-Coulomb model parameters are needed.

The model parameters are presented in Table 2.1. Only the SHANSEP parameters will be discussed in the present section. For the Mohr-Coulomb model parameters the reader may refer to Section 6.1.2 of the PLAXIS Reference Manual.

#### 2.1.1 SHANSEP PARAMETERS $\alpha$ AND $m$

Based on Eq. (2.1), the  $\alpha$  parameter represents the value of  $S_u/\sigma'_{v0}$  for a normally-consolidated soil ( $OCR = 1$ ). The power  $m$  is the value to which the *OCR* is raised. The magnitude of  $m$  represents the rate of strength increase with *OCR*.

Ladd & DeGroot (2003) indicate that for most clayey soil types,  $\alpha = 0.22 \pm 0.03$  and  $m = 0.80 \pm 0.1$ . Results of SHANSEP tests performed by Seah & Lai (2003) on soft Bangkok clay, which is a marine silty clay in the central area of Thailand, suggest the values of  $\alpha_c = 0.265$  and  $m_c = 0.735$  for compression tests and  $\alpha_c = 0.245$  and  $m_c = 0.890$  for

Table 2.1 SHANSEP MC model parameters

| Parameter                     | Symbol        | Description            | Unit |
|-------------------------------|---------------|------------------------|------|
| Mohr-Coulomb model parameters | $G$           | Shear modulus          | kPa  |
|                               | $\nu'$        | Poisson's ratio        | -    |
|                               | $c'$          | Cohesion               | kPa  |
|                               | $\phi'$       | Friction angle         | deg  |
|                               | $\psi$        | Dilatancy angle        | deg  |
|                               | $Tens$        | Tensile strength       | kPa  |
| SHANSEP parameters            | $\alpha$      | Coefficient            | -    |
|                               | $m$           | Power                  | -    |
|                               | $G/S_u$       | $G$ over $S_u$ ratio   | -    |
|                               | $S_{u_{min}}$ | Minimum shear strength | kPa  |
|                               | $OCR_{min}$   | Minimum $OCR$          | -    |

extension tests (see Eqs. (2.2) and (2.3)).

Santagata & Germaine (2002) studied the effects of sampling disturbance by conducting single element triaxial tests on normally-consolidated resedimented Boston blue clay (RBBC). The SHANSEP parameters obtained by undrained triaxial compression are  $\alpha = 0.33$  and  $m = 0.71$  for the intact RBBC, and  $\alpha = 0.33$  and  $m = 0.83$  for the disturbed RBBC.

Based on the studies presented above, it can be concluded that both SHANSEP  $\alpha$  and  $m$  parameters are stress path dependent. Even though the range of variation of the two SHANSEP parameters  $\alpha$  and  $m$  is not wide, the proper way to estimate them is via calibration of SHANSEP triaxial test results.

Figures 2.1 and 2.2 present the influence of both parameters on the normalised shear strength over the  $OCR$ . In Figure 2.1 the power  $m$  is constant and equal to 0.80, while the coefficient  $\alpha$  varies from 0.20 to 0.35. In Figure 2.2 the coefficient  $\alpha$  is constant and equal to 0.20, while the power  $m$  varies from 0.75 to 0.90. As expected, both parameters result in an increase of the undrained shear strength as they grow. Variation of the coefficient  $\alpha$  has greater influence on the resulting  $S_u/\sigma'_{v0}$ .

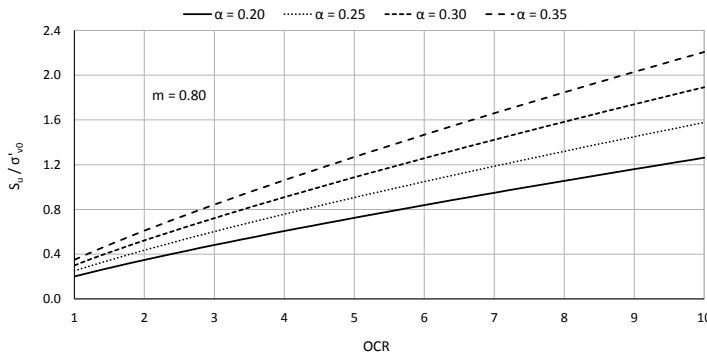


Figure 2.1 Influence of the coefficient  $\alpha$  on the normalised undrained shear strength



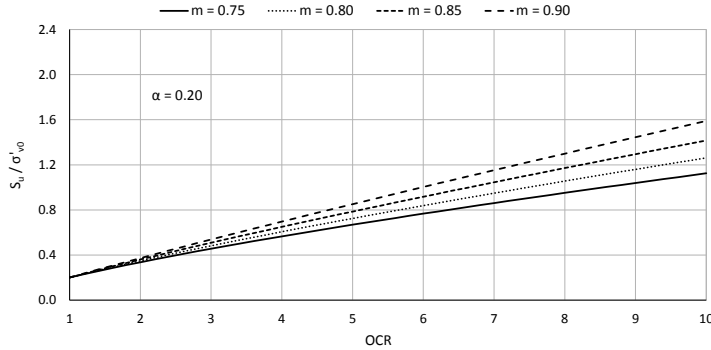


Figure 2.2 Influence of the power  $m$  on the normalised undrained shear strength

### 2.1.2 SHANSEP STIFFNESS PARAMETER

Soil stiffness is related to the undrained shear strength  $S_u$ , by adopting a constant ratio of the shear modulus  $G$  over  $S_u$ . The input parameter  $G/S_u$  allows to model the increase of stiffness with depth and thereby its variation with the current effective stress state.

Seah & Lai (2003) studied experimentally the undrained shear behaviour of soft Bangkok clay via undrained triaxial compression and extension tests. Based on the SHANSEP concept the following relationships between the shear modulus  $G_{50}$  and the undrained shear strength  $S_u$  were proposed:

$$\left(\frac{G_{50}}{S_u}\right)_{OC} = \frac{13(OCR)^{0.867}}{0.265(OCR)^{0.735}}, \quad \text{compression mode} \quad (2.2)$$

$$\left(\frac{G_{50}}{S_u}\right)_{OC} = \frac{8.1(OCR)^{0.708}}{0.245(OCR)^{0.890}}, \quad \text{extension mode} \quad (2.3)$$

Based on Termaat, Vermeer & Vergeer (1985), Figure 2.3 illustrates stiffness data for normally-consolidated clays. As it can be seen a typical range of the ratio  $G/S_u$  is between 50 and 250. This is in agreement with Duncan & Buchignani (1976), as presented in Figure 2.4 (considering  $E_u = 3G$ ). Eq. (2.4) is used for the fitting line presented in Figure 2.3.

$$\frac{G}{S_u} = \frac{5000}{I_p(\%)} \quad (2.4)$$

### 2.1.3 MINIMUM UNDRAINED SHEAR STRENGTH

To prevent zero or very small stiffness ( $G$ ) and strength ( $S_u$ ) at small depths where  $\sigma'_{v0}$  is equal to or approximately zero, a minimum value of the undrained shear strength  $S_{u_{min}}$  can be selected as input parameter. PLAXIS determines the value of  $S_u$  as:

$$S_u = \max(\alpha\sigma'_{v0}(OCR)^m, S_{u_{min}}) \quad (2.5)$$

A proper value for  $S_{u_{min}}$  can be determined from the field and/or laboratory characterization of the soil deposit. It is suggested that a value higher than the effective cohesion  $c'$  is selected, otherwise the analysis could be interrupted during the switching

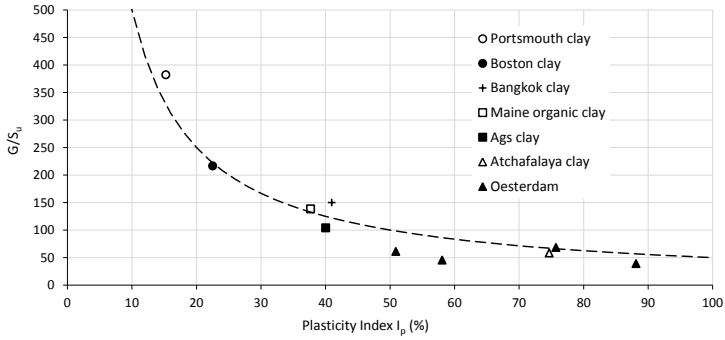


Figure 2.3 Relationship between  $G/S_u$  and  $I_p$  for normally consolidated clays,  $G$  is taken at 50 % strength (Termaat, Vermeer & Vergeer, 1985)

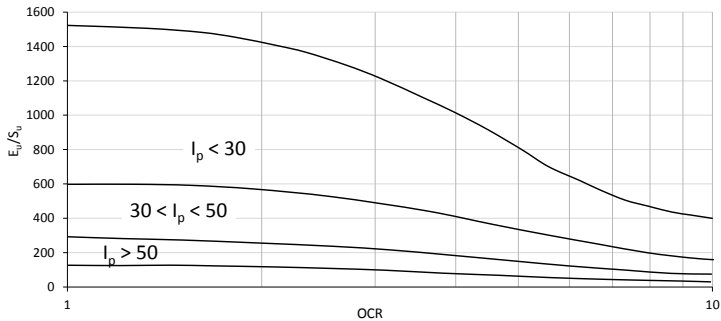


Figure 2.4 Relationship between  $E_u/S_u$  and  $OCR$  for different ranges of the Plasticity Index (Duncan & Buchignani, 1976)

to the SHANSEP MC model (see Section 2.2).

### 2.1.4 MINIMUM OVER-CONSOLIDATION RATIO

A minimum value of the  $OCR$  can be used as input value ( $OCR_{min}$ ). The purpose of this is to allow for an initial value of the pre-consolidation ratio higher than unity. During calculation, PLAXIS determines the current  $OCR$  as:

$$OCR = \max\left(\frac{\sigma'_{1,max}}{\sigma'_{1}}, OCR_{min}\right) \tag{2.6}$$

As PLAXIS calculation evolves,  $OCR$  can be updated by switching to the SHANSEP concept (see Section 2.2). In addition,  $OCR$  values from advanced soil models can be transferred to the SHANSEP MC model (see Section 2.4). This feature is available as from PLAXIS 2D 2016.01.

### 2.1.5 INTERFACES TABSHEET

The *Interfaces* tabsheet contains the material data for interfaces, i.e. the interface oedometer modulus,  $E_{oed}^{ref}$ , and the interface strength parameters  $c'_{inter}$ ,  $\phi'_{inter}$  and  $\psi_{inter}$ . Hence, the interface shear strength is directly given in strength parameters.

In addition, two parameters are included to enable stress-dependency of the interface stiffness according to a power law formulation:

$$E_{oed}(\sigma'_n) = E_{oed}^{ref} \left( \frac{\sigma'_n}{UD-P^{ref}} \right)^{UD-Power} \quad (2.7)$$

where UD-Power, is the rate of stress dependency of the interface stiffness, UD-P<sup>ref</sup> is the reference stress level (usually 100 kN/m<sup>2</sup>) and  $\sigma'_n$  is the effective normal stress in the interface stress point.

### 2.1.6 INITIAL TABSHEET

Based on the value of  $\phi'_{inter}$  selected in the *Interfaces* tabsheet, the lateral stress coefficient at rest  $K_0$  is automatically calculated as a default value to set up the initial horizontal stress:

$$K_0 = 1 - \sin(\phi'_{inter}) \quad (2.8)$$

This value may be changed by the user.

## 2.2 ON THE USE OF THE SHANSEP MC MODEL

The SHANSEP MC model is a user-defined soil model and can be selected through the *Material model* combo box in the *General* tabsheet. The reader may refer to Chapter 14 of the Material Models Manual for further study on the use of user-defined soil models (UDSM) in PLAXIS.

### 2.2.1 ON THE 'SWITCH' TO THE SHANSEP CONCEPT

The 'switch' to the SHANSEP concept is done by a certain file which is stored by the user within the project folder. This file should have the following format:

```
data.shansep.rs#
```

in which the special character # represents the calculation phase number at which the model is switched from the Mohr-Coulomb model to SHANSEP. The switch is done only for the activated materials. After the switch, the undrained shear strength  $S_u$  is calculated from Eq. (2.1) based on the current stress state and the maximum stress in the past, based on previous calculation phases or predefined input values. At the same time, the effective friction and dilation angles are reset to zero, while tension is still allowed.

After the first switch, the calculated undrained shear strength  $S_u$  is kept constant. The re-initiation of the  $S_u$  is possible if another 'SHANSEP file', which corresponds to a subsequent calculation phase, is stored within the project folder. The re-initiation can be done as many times as the user desires.

The SHANSEP MC model can also be used in the *Soil Test* facility. In this case, the switch has to be done directly at the beginning of the calculation. This is done by storing a file named 'data.shansep.rs0' within the directory where the files for the *Soil Test* are generated, i.e. %temp%\VL\_XXXX.

**Hint:** Depending on the user actions in the *Staged construction* mode, the number mentioned in the name of the calculation phase might be different than the actual number of this phase. For instance, this could happen if a new calculation phase is inserted or an already existing one is deleted. Therefore, it is better to verify the phase number, by writing the command 'echo phase\_#.number' in the command line, where 'phase\_#' stands for the phase ID.

## 2.2.2 STATE VARIABLES

The SHANSEP MC model provides output on two *State variables*. These parameters can be visualised by selecting the *State parameters* option from the *stresses* menu in the Output program. The *State variables* are:

*State variable 1:*  $\sigma'_{1,max}$  (compression is positive)

*State variable 2:*  $S_u$  (equals zero before the switch)

**Hint:** In order to create charts of the *State variables* via the *Curves manager* in the Output program, one or more stress points have to be selected after the calculation is completed (post-calculated stress points).

## 2.3 MODELLING THE UNDRAINED BEHAVIOUR

As mentioned in Section 2.1, the SHANSEP MC model should preferably have the drainage type set to Undrained (A). However, during the initial phase(s), before switching to the SHANSEP concept, undrained behaviour can be ignored by selecting the calculations option *Ignore undrained behaviour* in the *Phases* window. After switching to the SHANSEP concept (see Section 2.2), the model behaves similarly to the Undrained (B) Mohr-Coulomb model. However, as discussed below, the SHANSEP MC model is advantageous in comparison to the classic Undrained (B) drainage type of the Mohr-Coulomb model.

### 2.3.1 MOHR-COULOMB MODEL LIMITATIONS

In Undrained (B) calculations of PLAXIS, the Mohr-Coulomb model strength parameters are defined as  $c' = S_u$  and  $\phi' = 0^\circ$ . Thus, the Mohr-Coulomb criterion reduces to the more specific Tresca criterion, in which the undrained shear strength has a unique value, independent of the mean stress.

The Critical State Soil Mechanics defines the undrained shear strength as a negative exponential function of the specific volume:

$$S_u = \frac{M}{2} \exp\left(\frac{\Gamma - \nu}{\lambda}\right) \quad (2.9)$$

where  $M = q_{cs}/p'_{cs}$  is the stress ratio at the Critical State,  $\nu$  is the specific volume at the

Critical State (equal to the initial specific volume since an undrained path is followed),  $\Gamma$  and  $\lambda$  are the intercept and the slope of the Critical State Line respectively.

Based on Eq. (2.9), the undrained shear strength increases as the specific volume reduces. Hence, even in a homogenous soil deposit, the undrained shear strength increases with depth. This can be simulated with the Mohr-Coulomb model via the *Advanced parameters* option. Thus, the undrained shear strength is given by Eq. (2.10) for the Undrained (B) drainage type:

$$S_u(y) = S_{u_{ref}} + (y_{ref} - y) S_{u_{inc}} \quad y < y_{ref} \tag{2.10}$$

in which  $y$  stands for depth.

However, Eq. (2.10) is valid only in case that horizontal soil layers are considered. The reference depth ( $y_{ref}$ ) is a fixed value throughout the whole model. If the soil deposit is inclined (in case of slope, embankment etc.), according to Eq. (2.10), as depth increases, undrained shear strength increases as well along the surface. This leads to a non-realistic distribution of the undrained shear strength.

Figure 2.5 presents the Effective Stress Path (ESP) and the Total Stress Path (TSP) during undrained loading of soft normally-consolidated clays. If the drainage type is set to Undrained (A), the Effective Stress Path (ESP) is vertical in the  $p$ - $q$  plot ( $p'$  is constant) until failure. Hence, it over-estimates the undrained shear strength  $S_u$  and under-estimates the excess pore pressure  $p_w$ . If the drainage type is set to Undrained (B), an upper bound of the undrained shear strength  $S_u$  is pre-defined and constant. However, in this case, the model cannot take into account the variation of  $S_u$  caused by the change of the specific volume during the consolidation phases of a calculation.

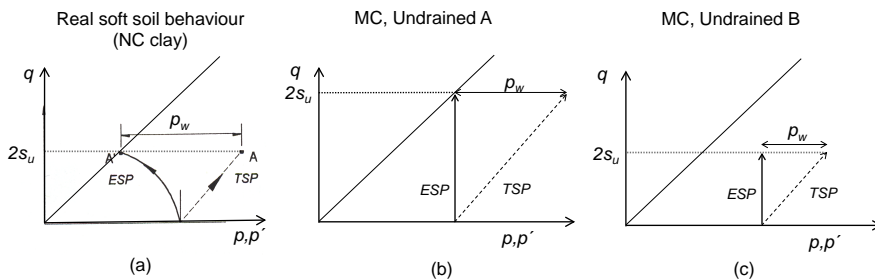


Figure 2.5 Undrained behaviour of real soft soil (a), Mohr-Coulomb model with Undrained (A) drainage type (b) and Mohr-Coulomb model with Undrained (B) drainage type (c)

### 2.3.2 THE ADVANTAGE OF THE SHANSEP MC MODEL

The SHANSEP MC model gives the advantage of a more realistic, empirical way of modelling the undrained shear strength  $S_u$ . Figure 2.6 illustrates a comparison between the real behaviour of a soft soil (a) and the SHANSEP MC concept (b) in terms of the ESP in  $p'$ - $q$  plot. During the first undrained loading the model behaves as Mohr-Coulomb model Undrained (A). A consolidation phase is introduced afterwards and the effective stress increases, reaching the Re-initiation Point 1 ( $RP_1$ ). At that point the switch to the SHANSEP model occurs (see Section 2.2) and the undrained shear strength is updated from its initial value  $S_u^{initial}$  to  $S_u^{updated\_1}$ . The same process is repeated again after the

next undrained loading and the subsequent consolidation, leading to the updated undrained shear strength  $S_u^{updated\_2}$ . This behaviour constitutes a better approach to reality in comparison with the standard Mohr-Coulomb model undrained behaviour (see Figure 2.5).

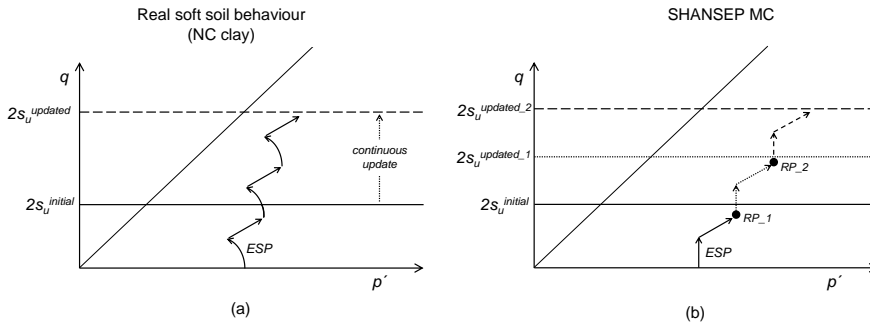


Figure 2.6 Undrained behaviour of real soft soil (a) and SHANSEP MC model (b)

**Hint:** It is suggested that the consolidation phase does not lead to deviatoric stress equal to the undrained shear strength, e.g. the Re-initiation Point 1 ( $RP_1$ ) in Figure 2.6 stays below the  $2S_u^{initial}$  cap. If the opposite occurs it is suggested to split the consolidation phase in more than one phases with shorter consolidation times and re-initiate the undrained shear strength after each one of them.

## 2.4 THE SHANSEP MC MODEL IN COMBINATION WITH OTHER CONSTITUTIVE MODELS

Apart from using the SHANSEP MC model merely as a Mohr-Coulomb model and then switching to the SHANSEP concept as described in Section 2.2, it is possible to use it as an 'extension' of any other constitutive model implemented in PLAXIS. This is particularly useful for the advanced models in which an over-consolidated stress state can be defined through the over-consolidation ratio:

- |                      |  |                         |
|----------------------|--|-------------------------|
| Hardening Soil model | Hardening Soil model with small-strain stiffness | Modified Cam-Clay model |
| Soft Soil model      | Soft Soil Creep model                            | Sekiguchi-Ohta model    |

To switch from an advanced soil model to the SHANSEP MC model the process described in Section 2.2 has to be followed. However, apart from the corresponding file needed to be stored in the project folder, the material of the soil cluster has also to be changed from the advanced model to the SHANSEP MC model.

To transfer the stress history from an advanced soil model to the SHANSEP MC model, two state parameters are used, namely the equivalent isotropic stress  $p_{eq}$  and the isotropic pre-consolidation stress  $p_p$  (refer to Section 9.3.5 of the PLAXIS Reference Manual).

Depending on the soil model, the equivalent isotropic stress  $p_{eq}$  is calculated as:

$$p_{eq} = \sqrt{p^2 + \frac{\tilde{q}^2}{\alpha^2}} \quad \text{for the Hardening Soil model and HS small model}$$

$$p_{eq} = p' - \frac{q^2}{M^2 (p' - c \cot \varphi)} \quad \text{for the Soft Soil model, Soft Soil Creep model and Modified Cam-Clay model. For the Modified Cam-Clay model, the cohesion } c \text{ is defined as } 0 \text{ kN/m}^2$$

$$p_{eq} = \frac{q}{\exp\left(-\frac{\tilde{q}}{Mp}\right)} \quad \text{for the Sekiguchi-Ohta model}$$

The isotropic pre-consolidation stress  $p_p$  represents the maximum equivalent isotropic stress level that a stress point has experienced up to the current load step. Based on these two state parameters, the *OCR* of the current calculation step is derived as:

$$OCR = \frac{p_p}{p_{eq}} \quad (2.11)$$

After switching to the SHANSEP MC model, based on the calculated *OCR* of the current step, the first SHANSEP state variable (see Section 2.2) is defined as:

$$\sigma'_{1,max} = OCR \cdot \sigma'_1 \quad (2.12)$$

To calculate the second state variable of the SHANSEP MC model, i.e. the undrained shear strength  $S_u$ , the result of Eq. (2.12) is used in combination with Eq. (2.1).





### 3 VERIFICATION - TRIAXIAL COMPRESSION TESTS

Triaxial compression tests were performed as a Finite Element calculation starting from three different initial stress states, i.e.  $\sigma'_{v0}$  equal to 200 kPa, 300 kPa and 400 kPa. In addition, four different over-consolidation ratios are considered, i.e.  $OCR$  equal to 1.2, 1.5, 1.8 and 2. Figure 3.1 illustrates the model geometry in PLAXIS 2D (a) and PLAXIS 3D (b). In PLAXIS 2D an axisymmetric model is used. A very coarse mesh is selected for both models. The boundary conditions are set to be *Normally fixed* for the left, bottom and rear (only for PLAXIS 3D) boundaries, while they are set to *Free* for every other boundary. Compressive loads are applied to the boundaries that are set to be *Free*.

Intention of the present example is to verify that the undrained shear strength is calculated correctly in PLAXIS after switching to the SHANSEP concept. The selected drainage type does not influence the results in terms of soil strength. Thus, the selected drainage type before switching to the SHANSEP MC model is not relevant and Drained material is used.

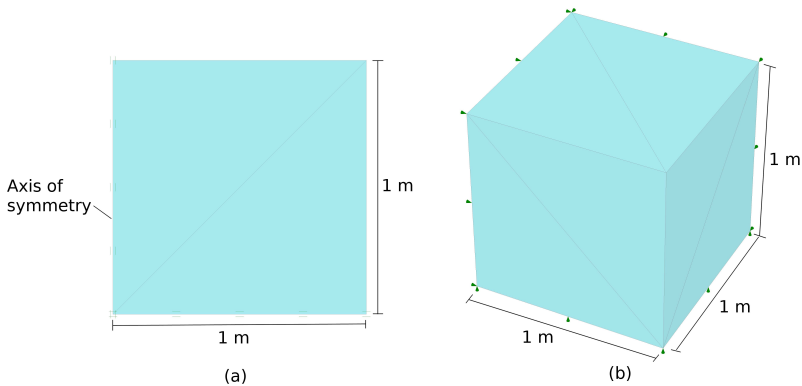


Figure 3.1 Model geometry in PLAXIS 2D (a) and PLAXIS 3D (b)

To obtain the desired  $OCR$  value an isotropic unloading phase follows the initial isotropic compression of the model. After the unloading, shear is applied via a prescribed displacement of 0.1 m at the top of the model. The resulting axial strain  $\epsilon_{\alpha}$  equals 10%. The SHANSEP MC input parameters adopted for the simulations are listed in Table 3.1.

Table 3.1 Adopted SHANSEP MC model parameters

| Symbol        | Value | Unit |
|---------------|-------|------|
| $G$           | 1000  | kPa  |
| $\nu'$        | 0.2   | -    |
| $c'$          | 1     | kPa  |
| $\phi'$       | 25    | deg  |
| $\psi$        | 0     | deg  |
| $Tens$        | 0     | kPa  |
| $\alpha$      | 0.2   | -    |
| $m$           | 0.8   | -    |
| $G/S_u$       | 200   | -    |
| $S_{u_{min}}$ | 1     | kPa  |
| $OCR_{min}$   | 1     | -    |

Table 3.2 presents a comparison between PLAXIS and the theoretically obtained results through Eq. (2.1) for all loading cases. The results are in perfect agreement.

Table 3.2 Comparison between PLAXIS and theoretical results

|                   |                |       | PLAXIS |                    | SHANSEP - Eq. (2.1) |                    |
|-------------------|----------------|-------|--------|--------------------|---------------------|--------------------|
| $\sigma'_{1,max}$ | $\sigma'_{v0}$ | $OCR$ | $S_u$  | $S_u/\sigma'_{v0}$ | $S_u$               | $S_u/\sigma'_{v0}$ |
| (kPa)             | (kPa)          | (-)   | (kPa)  | (-)                | (kPa)               | (-)                |
| 240               | 200            | 1.2   | 46.28  | 0.23               | 46.28               | 0.23               |
| 300               | 200            | 1.5   | 55.33  | 0.28               | 55.33               | 0.28               |
| 360               | 200            | 1.8   | 64.01  | 0.32               | 64.01               | 0.32               |
| 400               | 200            | 2.0   | 69.64  | 0.35               | 69.64               | 0.35               |
| 360               | 300            | 1.2   | 69.42  | 0.23               | 69.42               | 0.23               |
| 450               | 300            | 1.5   | 82.99  | 0.28               | 82.99               | 0.28               |
| 540               | 300            | 1.8   | 96.02  | 0.32               | 96.02               | 0.32               |
| 600               | 300            | 2.0   | 104.47 | 0.35               | 104.47              | 0.35               |
| 480               | 400            | 1.2   | 92.56  | 0.23               | 92.56               | 0.23               |
| 600               | 400            | 1.5   | 110.65 | 0.28               | 110.65              | 0.28               |
| 720               | 400            | 1.8   | 128.03 | 0.32               | 128.03              | 0.32               |
| 800               | 400            | 2.0   | 139.29 | 0.35               | 139.29              | 0.35               |

Figure 3.2 illustrates the variation of the normalised shear strength  $S_u$  over the corresponding vertical effective stress  $\sigma'_{v0}$  against  $OCR$ . PLAXIS 2D and PLAXIS 3D results are in perfect match. The fitting power line result in an equation which is in perfect agreement with Eq. (2.1) for the adopted SHANSEP parameters, i.e.  $\alpha = 0.2$  and  $m = 0.8$ . The undrained shear strength increases with increasing  $OCR$ .

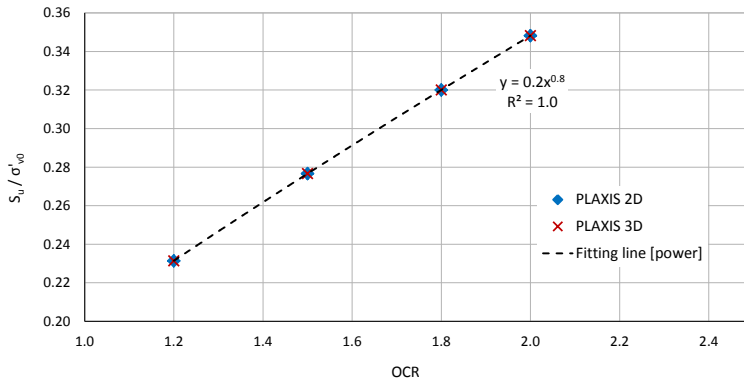


Figure 3.2  $S_u/\sigma'_{v0}$  over  $OCR$  obtained in PLAXIS

Figure 3.3 presents the deviatoric stress  $q$  normalised over the vertical effective stress  $\sigma'_{v0}$  against the axial strain, for each one of the studied loading cases (see Table 3.2). The results are plot for all studied  $OCR$  values as well. There is perfect agreement between the cases which have different pre-consolidation and current effective stresses, but the same  $OCR$ . Thus, each one of the lines depicted in Figure 3.3 consists of three lines plot on top of each other.

The obtained undrained shear strength in PLAXIS is verified analytically with Eq. (3.1) and the analytical results are in perfect agreement with the results presented in Figure

3.3.

$$q_{max} = 2S_u \quad (3.1)$$

An additional verification check is related to the inclination of the loading branch of each line presented in Figure 3.3 and the axial strain at which the perfectly plastic behaviour starts. The inclination equals the effective Young's modulus  $E'$ , while the perfectly plastic behaviour starts at the yield strain  $\epsilon_y$ :

$$E' = 2G(1 + \nu') = 400S_u(1 + \nu'), \quad (\text{for } G = 200S_u) \quad (3.2)$$

$$\epsilon_y = \frac{q_{max}}{E'} = \frac{2S_u}{E'} \quad (3.3)$$

Both values depend on the undrained shear strength  $S_u$ . PLAXIS results are in perfect agreement with the analytically calculated  $E'$  and  $\epsilon_y$ .

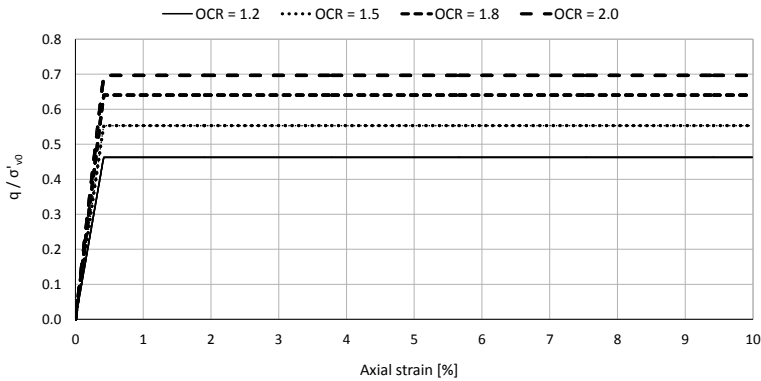


Figure 3.3 PLAXIS results for the normalised deviatoric stress  $q$  against the axial strain, for all studied  $OCR$  values

For the loading case with  $OCR$  equal to 2 and vertical effective stress equal to 200 kPa, a parametric analysis is performed by varying the SHANSEP parameters  $\alpha$  and  $m$ . In one case,  $m$  is set equal to 0.8 while  $\alpha$  varies from 0.20 to 0.30. In the second case,  $\alpha$  is set equal to 0.2 while  $m$  varies from 0.80 to 0.90. Figures 3.4 and 3.5 present the corresponding results. As concluded in Section 2.1, in both cases increase of the SHANSEP parameters results in higher undrained shear strength. Variation of the parameter  $\alpha$  influences the result more.

Figure 3.6 compares the results between PLAXIS 2D and the *Soil Test* facility (see Section 2.2) for the loading case with  $OCR$  equal to 1.2 and vertical effective stress equal to 200 kPa. Both tests result in the same undrained shear strength.

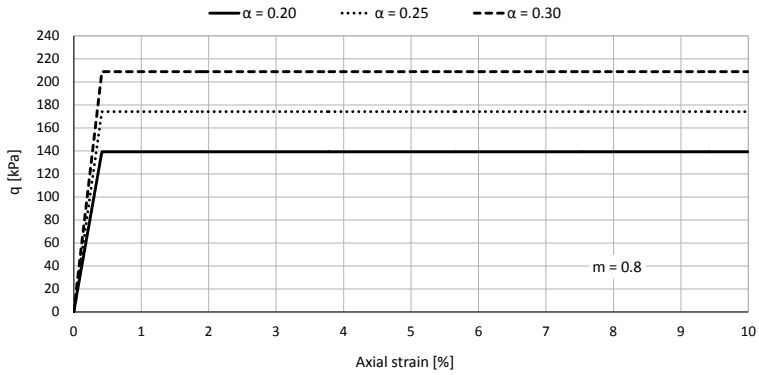


Figure 3.4 Influence of the parameter  $\alpha$  on the undrained shear strength

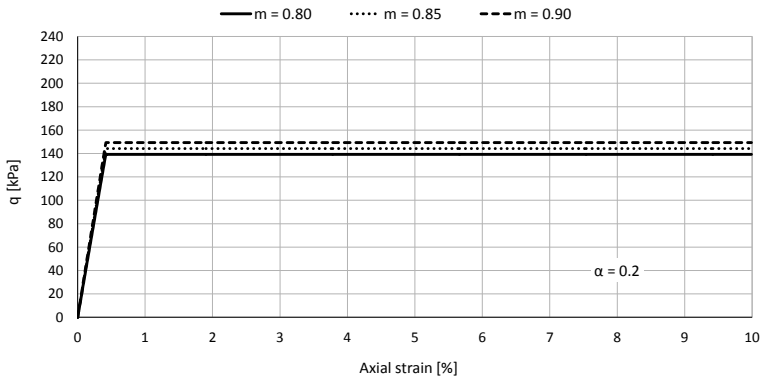


Figure 3.5 Influence of the parameter  $m$  on the undrained shear strength

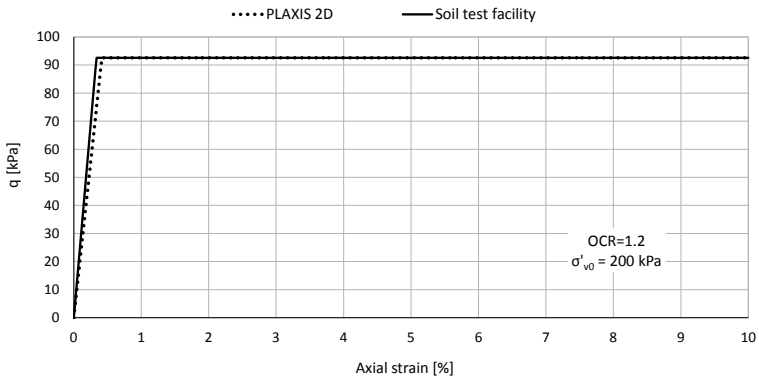


Figure 3.6 Comparison between Finite Element calculation and *Soil Test* facility

## 4 PRACTICAL APPLICATIONS

### 4.1 FLUCTUATION OF THE PHREATIC LEVEL

The seasonal fluctuation of the phreatic level in a submerged slope is simulated to evaluate the effect of the varying *OCR* due to the water level fluctuation on the slope stability. A plain-strain model is used in PLAXIS 2D with dimensions equal to 60 m in the horizontal x-direction and 25 in the vertical y-direction. Figure 4.1 illustrates the model geometry. The slope is 30 long and 13 m tall. The water level is initially set at its average level, i.e. 'Level 1', which is 9 m above the height of the toe. The water level fluctuation equals  $\pm 3$  m, thus 'Level 2' equals 12 m and 'Level 3' equals 6 m. The standard boundary conditions are used for deformations and ground water flow (also for consolidation purposes). Undrained behaviour is considered. The *Very fine* option is selected for the *Element distribution*. The generated mesh is illustrated in Figure 4.1 as well.

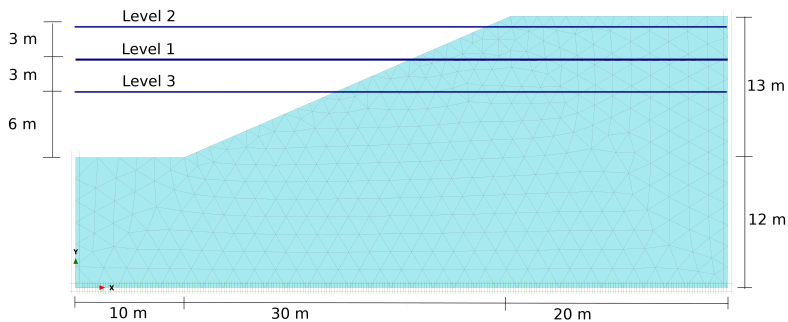


Figure 4.1 Model geometry and generated mesh in PLAXIS 2D

The soil deposit is homogenous and the material properties are listed in Table 4.1. The SHANSEP parameters  $\alpha$  and  $m$  are chosen based on the normalized behaviour of disturbed resedimented Boston blue clay (RBBC), as reported by Santagata & Germaine (2002).

Table 4.1 Adopted SHANSEP MC model parameters

| Symbol           | Value               | Unit              |
|------------------|---------------------|-------------------|
| $\gamma_{unsat}$ | 17                  | kN/m <sup>3</sup> |
| $\gamma_{sat}$   | 20                  | kN/m <sup>3</sup> |
| $k_x$            | $1.0 \cdot 10^{-4}$ | m/day             |
| $k_y$            | $5.0 \cdot 10^{-5}$ | m/day             |
| $G$              | 1200                | kPa               |
| $\nu'$           | 0.2                 | -                 |
| $c'$             | 5                   | kPa               |
| $\phi'$          | 23                  | deg               |
| $\psi$           | 0                   | deg               |
| $Tens$           | 0                   | kPa               |
| $\alpha$         | 0.33                | -                 |
| $m$              | 0.83                | -                 |
| $G/S_u$          | 200                 | -                 |
| $S_{u_{min}}$    | 5                   | kPa               |
| $OCR_{min}$      | 1                   | -                 |

The *Gravity loading* calculation type is used to generate the initial stress state, with the phreatic level placed at Level 1 (average level). For the *Gravity loading* calculation type the option *Ignore undrained behaviour* is automatically selected in the *Phases* window. For all subsequent calculation phases undrained behaviour is considered. In Phase 1, an increase of the water level up to Level 2 is simulated with a plastic phase. A consolidation phase follows (Phase 2), in which the *Minimum excess pore pressure* loading type is used and a minimum value of excess pore pressures (1 kN/m<sup>2</sup>) is reached throughout the whole model. Subsequently, the water level is set to Level 1 again and the same phase sequence is followed (Phase 3 is plastic analysis and Phase 4 is consolidation to minimum excess pore pressures). Afterwards, the water level is set to Level 3 and once more the same phase sequence is adopted (Phase 5 is plastic analysis and Phase 6 is consolidation to minimum excess pore pressures). For the last two calculation phases the water level is placed again at Level 1 and the same phase sequence is adopted (Phase 7 is plastic analysis and Phase 8 is consolidation to minimum excess pore pressures). After each consolidation phase a safety analysis is conducted and the global safety factor is computed.

The switch to the SHANSEP model occurs in Phase 1. In this way, the calculation is not affected by the over-estimation of the shear strength due to the Undrained (A) Mohr-Coulomb model (see Section 2.3). The shear strength is re-initiated after every consolidation phase, i.e. at Phases 3, 5 and 7.

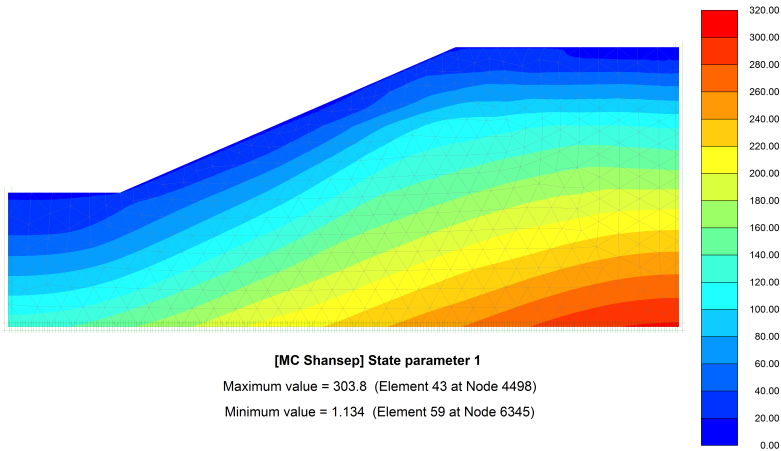
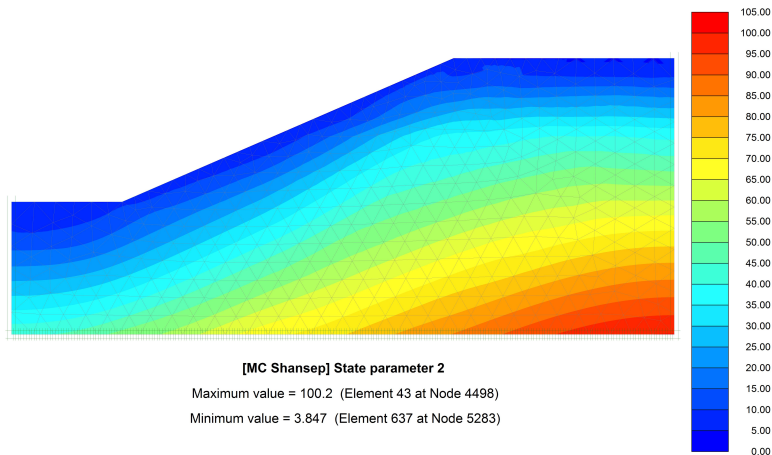
Table 4.2 presents the results of each calculation phase for the stress point in which the maximum stress occurs (right-bottom of the model). The phases in which there is the updating of the strength are marked with an asterisk. Figures 4.2 and 4.3 illustrate an example of state parameter 1 ( $\sigma'_{1,max}$ ) and state parameter 2 ( $S_u$ ) variation throughout the whole model after the last consolidation phase (Phase 8).

Table 4.2 PLAXIS calculation results

| Phase   | $\sigma'_{1,max}$<br>(kPa) | $\sigma'_1$<br>(kPa) | $\sigma'_{v0}$<br>(kPa) | <i>OCR</i><br>(-) | $S_u$<br>(kPa) | $S_u/\sigma'_{v0}$<br>(-) |
|---------|----------------------------|----------------------|-------------------------|-------------------|----------------|---------------------------|
| Initial | 281.0                      | 281.0                | 281.0                   | 1.00              | 0.0            | 0.00                      |
| 1*      | 281.0                      | 208.5                | 208.5                   | 1.00              | 92.72          | 0.33                      |
| 2       | 281.0                      | 259.2                | 259.2                   | 1.08              | 92.72          | 0.35                      |
| 3*      | 281.0                      | 259.6                | 259.6                   | 1.08              | 91.46          | 0.35                      |
| 4       | 281.0                      | 279.8                | 279.8                   | 1.00              | 91.46          | 0.33                      |
| 5*      | 281.0                      | 280.3                | 280.3                   | 1.00              | 92.66          | 0.33                      |
| 6       | 303.8                      | 303.8                | 303.8                   | 1.00              | 92.66          | 0.31                      |
| 7*      | 303.8                      | 303.8                | 303.8                   | 1.00              | 100.20         | 0.33                      |
| 8       | 303.8                      | 282.4                | 282.4                   | 1.08              | 100.20         | 0.35                      |

The material is initially normally-consolidated and when the water level increases (Phase 1), it experiences the first unloading of its stress history. The resulting higher *OCR* (1.08) leads to an increase of the ratio  $S_u/\sigma'_{v0}$  from 0.33 in Phase 1 to 0.35 in Phase 3. For the same phases,  $\sigma'_{v0}$  reduces from 280.5 kPa to 259.6 kPa. Thus, the observed increase of the normalised shear strength is a function of the *OCR*, based on Eq. (2.1). However, the actual  $S_u$  value decreases compared to the previous phases due to the reduced stress level.

In Phases 5 and 6 the water table is at the lowest level (Level 3). The effective stress state increases and the previous  $\sigma'_{1,max}$  is overcome after the consolidation in Phase 6. The re-initiation of the shear strength in the following phase (Phase 7) shows an increase of  $S_u$  as there is an increase of  $\sigma'_{v0}$ , even though the material is still normally

Figure 4.2 State parameter 1 ( $\sigma'_{1,max}$ ), Phase 8 (units in kPa)Figure 4.3 State parameter 2 ( $S_u$ ), Phase 8 (units in kPa)

consolidated ( $OCR = 1.00$ ).

In both Phases 4 and 8 the water table is at Level 1. However, the  $OCR$  and the undrained shear strength  $S_u$  are higher in Phase 8. This is because between those two phases the water level decreases leading to an increase of the effective stresses throughout the soil deposit. Both  $OCR$  and  $S_u$  are affected by the soil stress history.

Figure 4.4 illustrates the results of the safety analyses after every consolidation phase. The number in brackets when the water table is at Level 1 indicates the passing sequence, i.e. [1] stands for the first passing (from Level 2 to Level 1 in Phase 3) and [2] stands for the second passing (from Level 3 to Level 1 in Phase 7). The fluctuation of the water level causes variation of the global Factor of Safety (FoS). The latter is calculated in

PLAXIS as:

$$FoS = \frac{S_u^{input}}{S_u^{equilibrium}} \tag{4.1}$$

When the water table is at the highest level (Level 2) the water load applied at the slope acts as an extra balance force and assists equilibrium. The FoS equals 1.408 in this case. When the water level reduces to Level 1 and then Level 3, the undrained shear strength does not change significantly (see Table 4.2) but the balance force induced by the water load diminishes. As a result, the FoS equals 1.159 and 1.022 correspondingly. By comparing the results when the water table is at Level 1, the FoS is higher in case of the second passing (1.381). In both cases the water load acting on the slope is the same, but in the second passing (Phase 8), the undrained shear strength is higher (see Table 4.2).

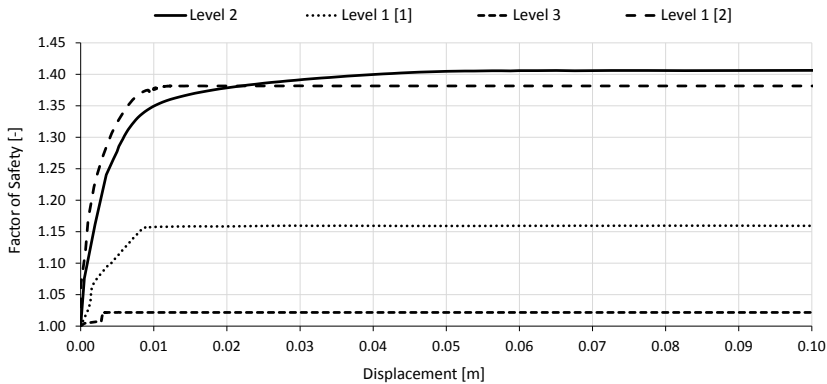


Figure 4.4 Factor of Safety according to the various water levels

Assuming the same project, if the minimum value of the  $OCR$  was selected equal to 2 ( $OCR_{min} = 2$ ), the variation of the undrained shear strength would merely be affected by the variation of the vertical effective stress  $\sigma'_{v0}$ , as the water fluctuation does not lead to an  $OCR$  higher than the predefined minimum value. Figure 4.5 illustrates the variation of the normalised undrained shear strength over the project phases. The higher  $OCR_{min}$  leads to higher undrained shear strength.



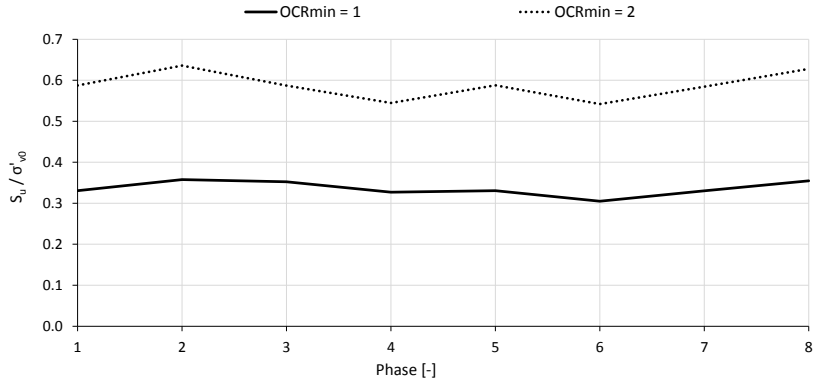


Figure 4.5 Normalised undrained shear strength over project phases for different predefined values of  $OCR_{min}$

## 4.2 EMBANKMENT CONSTRUCTION ON SOFT CLAY

The construction of an embankment is simulated to compare the results between the SHANSEP MC model and the Undrained (B) Mohr-Coulomb model. A plain-strain model is used in PLAXIS 2D. Since the geometry is considered symmetric, only half of the embankment is modeled and the drainage is prevented only through the plane of symmetry (left model boundary), while the standard boundary conditions for deformations are adopted. The model length equals 35 m in the horizontal x-direction. The height of the initial soil deposit (without the embankment) equals 7 m. The water level is set 1 m below the top soil surface.

The embankment is built in stages. Its slope equals 1:1.5 (height:length). After the last top layer of the embankment is constructed, part of the initial soil deposit together with the top layer of the embankment are excavated. The purpose of the excavation is to cause an over-consolidated soil state. In between the various model geometry changes *Consolidation* phases are added with consolidation time equal to 60 days in order to allow for excess pore pressure dissipation. Afterwards a load equal to 8 kN/m/m with length of 3 m is applied on top of the embankment. A *Consolidation* phase to minimum excess pore pressures equal to 1 kN/m<sup>2</sup> follows. The last calculation phase is a safety analysis.

The *Very fine* option is selected for the *Element distribution*. Figure 4.6 illustrates the model geometry and the generated mesh. The soil clusters numbering from 1 to 4 is used in Table 4.3 to clarify the staged construction phases.

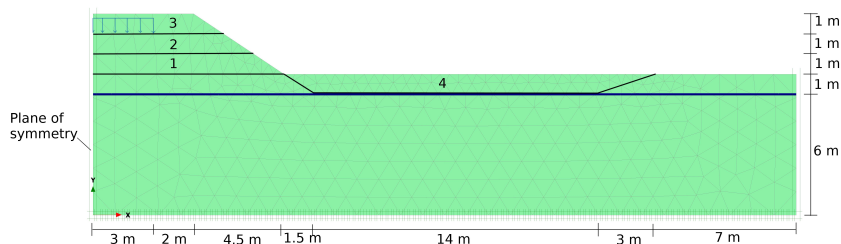


Figure 4.6 Model geometry and generated mesh in PLAXIS 2D

Table 4.3 Staged construction details

| Phase   | Calculation type     | Time (days) | Staged construction details       |
|---------|----------------------|-------------|-----------------------------------|
| Initial | <i>K0 procedure</i>  | -           | Deactivated soil clusters 1, 2, 3 |
| 1       | <i>Consolidation</i> | 1           | Activate soil cluster 1           |
| 2       | <i>Consolidation</i> | 60          | -                                 |
| 3       | <i>Consolidation</i> | 1           | Activate soil cluster 2           |
| 4       | <i>Consolidation</i> | 60          | -                                 |
| 5       | <i>Consolidation</i> | 1           | Activate soil cluster 3           |
| 6       | <i>Consolidation</i> | 60          | -                                 |
| 7       | <i>Consolidation</i> | 1           | Deactivate soil clusters 3 and 4  |
| 8       | <i>Consolidation</i> | 60          | -                                 |
| 9       | <i>Consolidation</i> | 1           | Activate load                     |
| 10      | <i>Consolidation</i> | Unspecified | Min $p_{excess}$                  |
| 11      | <i>Safety</i>        | -           | -                                 |

The soil deposit is homogenous and the material properties are listed in Table 4.4. Undrained behaviour is considered. The SHANSEP parameters  $\alpha$  and  $m$  are chosen based on the soft Bangkok clay undrained triaxial compression tests as reported by Seah & Lai (2003). The switch to the SHANSEP model occurs in Phase 1. The shear strength is re-initiated after every next phase from Phase 2 to Phase 11.

Table 4.4 Adopted SHANSEP MC model parameters

| Symbol           | Value               | Unit              |
|------------------|---------------------|-------------------|
| $\gamma_{unsat}$ | 13                  | kN/m <sup>3</sup> |
| $\gamma_{sat}$   | 15                  | kN/m <sup>3</sup> |
| $k_x$            | $1.0 \cdot 10^{-4}$ | m/day             |
| $k_y$            | $5.0 \cdot 10^{-5}$ | m/day             |
| $G$              | 1172                | kPa               |
| $\nu'$           | 0.33                | -                 |
| $c'$             | 7                   | kPa               |
| $\phi'$          | 23                  | deg               |
| $\psi$           | 0                   | deg               |
| $Tens$           | 0                   | kPa               |
| $\alpha$         | 0.265               | -                 |
| $m$              | 0.735               | -                 |
| $G/S_u$          | 150                 | -                 |
| $S_{u_{min}}$    | 7                   | kPa               |
| $OCR_{min}$      | 1                   | -                 |

Intention of the present example is to compare the SHANSEP MC results with the standard Mohr-Coulomb model results. For that purpose the Undrained (B) model is calibrated such that the selected material properties in terms of stiffness and strength are suitable for comparison. This is done based on the resulting undrained shear strength  $S_u$  of the SHANSEP MC model as it is re-initiated at the last calculation phase (Phase 11). Figure 4.7 depicts the  $S_u$  variation over the whole model at the beginning of Phase 11.

To derive the Undrained (B) Mohr-Coulomb model parameters based on Figure 4.7, an average value is estimated for the  $S_u$ , which increases with depth. Thus, a reference height ( $y_{ref}$ ) equal to 7 m is selected at which  $S_u$  equals 7 kPa. The  $S_u$  increases towards the bottom of the model, with a rate of  $S_{u_{inc}} = 0.45$  kPa/m, and it reaches a maximum value of 9.7 kPa at the bottom.

Since stiffness is linked to the variation of the  $S_u$  via the input parameter  $G/S_u = 150$ , the stiffness of the Mohr-Coulomb model has to be adjusted as well. Based on the adopted

$S_u$  profile, the shear modulus  $G$  is back-calculated. The variation of the stiffness profile is adjusted in the Mohr-Coulomb model by changing the Young's modulus  $E'$ . The latter is calculated based on Eq. (3.2). Table 4.5 presents the adopted model parameters for the Undrained (B) Mohr-Coulomb model.

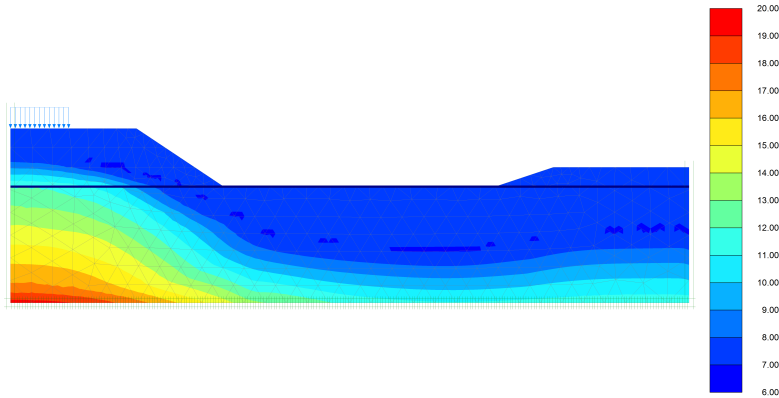


Figure 4.7 Undrained shear strength at the beginning of Phase 11 (units in kPa)

Table 4.5 Adopted Undrained (B) Mohr-Coulomb model parameters

| Symbol           | Value               | Unit              |
|------------------|---------------------|-------------------|
| $\gamma_{unsat}$ | 13                  | kN/m <sup>3</sup> |
| $\gamma_{sat}$   | 15                  | kN/m <sup>3</sup> |
| $k_x$            | $1.0 \cdot 10^{-4}$ | m/day             |
| $k_y$            | $5.0 \cdot 10^{-5}$ | m/day             |
| $E'$             | 2793                | kPa               |
| $E'_{inc}$       | 150                 | kPa/m             |
| $S_u$            | 7                   | kPa               |
| $S_{u,inc}$      | 0.45                | kPa/m             |
| $y_{ref}$        | 7                   | m                 |
| $\nu'$           | 0.33                | -                 |
| $\phi_u$         | 0                   | deg               |
| $\psi$           | 0                   | deg               |

In order to compare the results, the settlement at a point under the embankment is considered. The selected point is located 1 m at the right of the plane of symmetry, at height equal to 7 m. Figure 4.8 presents the results. As the plot indicates, the stiffness variation is well adjusted in the Undrained (B) Mohr-Coulomb model. At the first two phases (construction and consolidation of the soil cluster 1) the applied load through the added soil deposit is low and the soil behaves mainly elastically. Both models give similar results. The correctness of the selected stiffness is also verified through the total consolidation time needed till the end of Phase 10. The consolidation time is inversely proportional to the soil stiffness given that permeability is the same. The total consolidation time equals about 1310 days in both cases.

Regarding the soil strength, both models result in the same vertical displacement at the end of Phase 10. However, their behaviour is much different during the intermediate phases. This is explained by the fact that the Mohr-Coulomb model strength was adjusted based on the resulting undrained shear strength of the SHANSEP MC model at the last phase of the calculation. In the SHANSEP calculation, the undrained shear

strength is continuously updated after every consolidation phase. Thus, the strength is low at the beginning and increases as the load history evolves. As a result, the Mohr-Coulomb model has stiffer behaviour which is constant throughout the whole calculation, while the SHANSEP MC model gradually increases its stiffness.

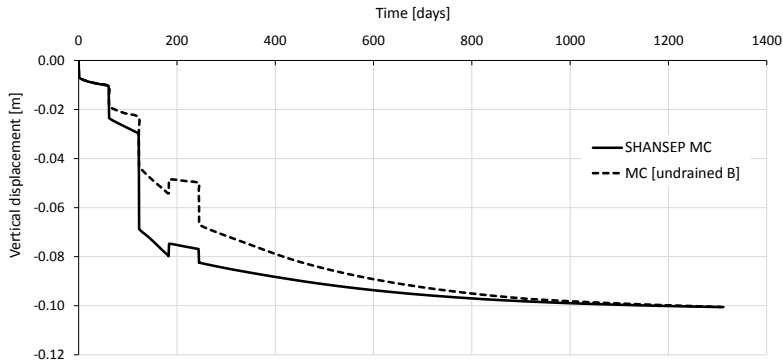


Figure 4.8 Comparison between SHANSEP MC and Undrained (B) Mohr-Coulomb model settlement results

Figure 4.9 presents a comparison of the computed Factors of Safety (FoS) for both models. For the SHANSEP MC model the FoS equals 1.166, while for the Mohr-Coulomb model equals 1.004. The explanation of such a difference between the Factors of Safety lies on the  $S_u$  updated profile of the SHANSEP MC model. Figures 4.10 and 4.11 illustrate the corresponding failure mechanisms. As it can be seen the failure mechanism in case of the Mohr-Coulomb model goes much deeper into the soil deposit. On the contrary, the failure mechanism for the SHANSEP MC model is much shallower. This is because of the  $S_u$  profile as depicted in Figure 4.7. Due to the adopted load history (especially after the deactivation of two soil clusters in Phase 7), the undrained shear strength increases below the embankment. Because of the  $S_u$  profile the slip surface is 'forced' closer to the slope, resulting in higher Factor of Safety.

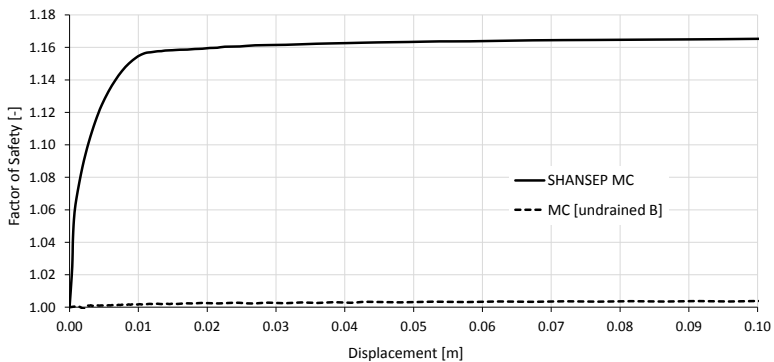


Figure 4.9 Comparison between SHANSEP MC and Undrained (B) Mohr-Coulomb model Factor of Safety results



Figure 4.10 Failure mechanism for the SHANSEP MC model



Figure 4.11 Failure mechanism for the Undrained (B) Mohr-Coulomb model

### 4.3 THE SHANSEP MC AND THE SOFT SOIL CREEP MODEL

The settlement below an embankment due to creep is simulated in order to study its effects on the Factor of Safety (FoS). A plain-strain model is used in PLAXIS 2D. Since the geometry is considered symmetric, only half of the embankment is modeled. The standard boundary conditions for the deformations are adopted. The model length equals 35 m in the horizontal x-direction. The height of the initial soil deposit (without the embankment) equals 7 m. The embankment is 3 m tall with slope of 1:1.5 (height:length). The *Very fine* option is selected for the *Element distribution*. Figure 4.12 illustrates the model geometry and the generated mesh.

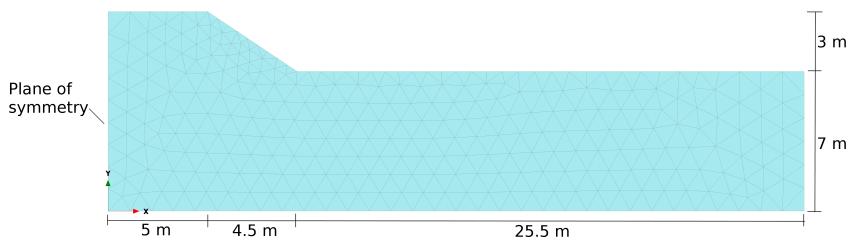


Figure 4.12 Model geometry and generated mesh in PLAXIS 2D

The Soft Soil Creep model is used to simulate the soil deposit. The adopted material properties are presented in Table 4.6.

Each calculation phase corresponds to different time period, i.e. 10 days, 100 days, 1000 days, 10000 days and 100000 days. The calculation type is *Plastic* analysis. Drained behaviour is considered. After a calculation phase with the Soft Soil Creep model is finished, an extra calculation phase is added in order to switch from the Soft Soil Creep model to the SHANSEP MC model (see Section 2.2). The undrained shear strength is re-initiated as the stress history is transferred from the Soft Soil Creep model to the SHANSEP MC model, as described in Section 2.4. A safety analysis follows in order to

Table 4.6 Adopted material properties for the Soft Soil Creep model

| Symbol           | Value  | Unit              |
|------------------|--------|-------------------|
| $\gamma_{unsat}$ | 15     | kN/m <sup>3</sup> |
| $\gamma_{sat}$   | 17     | kN/m <sup>3</sup> |
| $\lambda^*$      | 0.105  | -                 |
| $\kappa^*$       | 0.016  | -                 |
| $\mu^*$          | 0.004  | -                 |
| $c'_{ref}$       | 5      | kPa               |
| $\phi'$          | 32     | deg               |
| $\psi$           | 0      | deg               |
| $\nu'_{ur}$      | 0.15   | -                 |
| $K_0^{nc}$       | 0.4701 | -                 |

calculate the FoS for the various considered time periods.

The adopted material properties for the SHANSEP MC model are presented in Table 4.7.

Table 4.7 Adopted SHANSEP MC model parameters (drained behaviour)

| Symbol           | Value | Unit              |
|------------------|-------|-------------------|
| $\gamma_{unsat}$ | 15    | kN/m <sup>3</sup> |
| $\gamma_{sat}$   | 17    | kN/m <sup>3</sup> |
| $G$              | 770   | kPa               |
| $\nu'$           | 0.3   | -                 |
| $c'$             | 5     | kPa               |
| $\phi'$          | 32    | deg               |
| $\psi$           | 0     | deg               |
| $Tens$           | 0     | kPa               |
| $\alpha$         | 0.33  | -                 |
| $m$              | 0.83  | -                 |
| $G/S_u$          | 150   | -                 |
| $S_{u,min}$      | 5     | kPa               |
| $OCR_{min}$      | 1     | -                 |

Figure 4.13 illustrates the FoS evolution over time. As time increases, the isotropic pre-consolidation stress  $p_p$  increases, while the equivalent isotropic stress  $p_{eq}$  remains unchanged. Thus, based on Eq. (2.11), the  $OCR$  increases. As discussed in Section 2.4, the undrained shear strength increases as well. After each switch to the SHANSEP MC model, the undrained shear strength is re-initiated, leading to higher FoS as time increases.

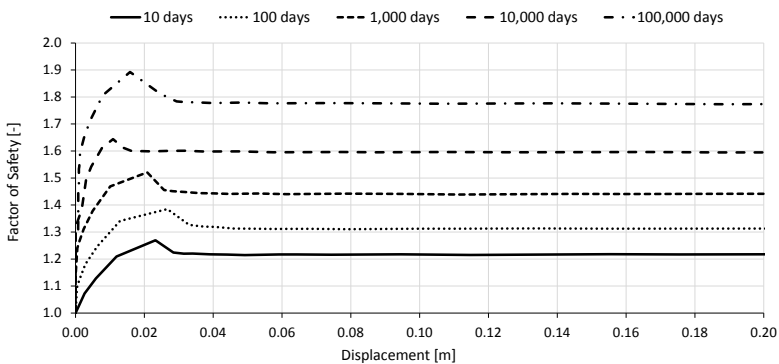


Figure 4.13 Factor of Safety evolution over time

## 5 CONCLUSIONS

The SHANSEP MC model is a constitutive model developed to overcome limitations of the traditional MC model related to the undrained shear strength of soils. Five additional input parameters are needed for this model, namely  $\alpha$ ,  $m$ ,  $G/S_u$ ,  $S_{u_{min}}$  and  $OCR_{min}$ . The model is based on the SHANSEP concept, which describes the undrained shear strength as a function of the effective stress history. Moreover, via the parameter  $G/S_u$  the dependence of the shear stiffness on the undrained shear strength is taken into account.

The two SHANSEP parameters  $\alpha$  and  $m$  influence the value of the undrained shear strength. The effect of these parameters was investigated and the results show that the effect of  $\alpha$  is more predominant. However, the range of variation of these two parameters is short.

Comparison between numerical results and analytical solutions during undrained triaxial compression tests starting from different initial vertical effective stress and  $OCR$  verifies that the model is well implemented in PLAXIS.

Three practical applications were performed to show how the model features influence the soil behavior. In the first practical case, the fluctuation of the water level and its influence on the undrained shear strength is studied. In the second application, it is proven that the stress history during an embankment construction affects the variation of the undrained shear strength and the corresponding Factors of Safety. In the third case, a way of using the SHANSEP MC model in combination with advanced soil models is demonstrated.





## 6 REFERENCES

- [1] Duncan, J.M., Buchignani, A.L. (1976). An engineering manual for settlement studies. University of California, Department of Civil Engineering.
- [2] Henkel, D.J. (1960). The shear strength of saturated remolded clays. In Proceedings of the ASCE Specialty Conference on Shear Strength of Cohesive Soils. University of Colorado, Boulder, 533–554.
- [3] Ladd, C.C., DeGroot, D.J. (2003). Recommended practice for soft ground site characterization: Arthur casagrande lecture. In Proceedings of the 12th Panamerican Conference on Soil Mechanics and Geotechnical Engineering, Massachusetts Institute of Technology, Cambridge, MA, USA.
- [4] Ladd, C.C., Foott, R. (1974). New design procedure for stability of soft clays. *Journal of the Geotechnical Engineering Division*, 100(7), 763–786.
- [5] Parry, R.H.G. (1960). Triaxial compression and extension tests on remoulded saturated clay. *Géotechnique*, 10(4), 166–180.
- [6] Santagata, M.C., Germaine, J.T. (2002). Sampling disturbance effects in normally consolidated clays. *Journal of Geotechnical and Geoenvironmental Engineering*, 128(12), 997–1006.
- [7] Seah, T.H., Lai, K.C. (2003). Strength and deformation behavior of soft bangkok clay. *Geotechnical Testing Journal*, 26(4), 421–431.
- [8] Termaat, R.J., Vermeer, P.A., Vergeer, C.J.H. (1985). Failure by large plastic deformations. In Proceedings of the 11th International Conference on Soil Mechanics and Foundation Engineering, San Francisco, 12-16 Aug.

